Dynamics of Gold Droplet Formation on SiO 2 /Si(111) Surface

Hadi Hijazi, Frédéric Leroy, Guillaume Monier, Gabin Grégoire, Evelyne Gil, Agnès Trassoudaine, Vladimir G Dubrovskii, Dominique Castelluci, Nebile Isik Goktas, Ray Lapierre, et al.

Dynamics of Au Droplet Formation on SiO_2/Si(111) Surface

Hadi Hijazi [†,‡,*], *Frédéric Leroy* [§], *Guillaume Monier* [†], *Gabin Grégoire* [†], *Evelyne Gil* [†,‡], *Agnès Trassoudaine* [†], *Vladimir G. Dubrovskii* [‡], *Dominique Castelluci* [†], *Nebile Isik Goktas*[‖], *Ray R. LaPierre* [‖], *Yamina André* [†,‖], *Christine Robert-Goumet* [†]

[†]*Université Clermont Auvergne, CNRS, SIGMA Clermont, Institut Pascal, F-63000 Clermont-Ferrand, France.*

[‡] *ITMO University, Kronverkskiy pr. 49, 197101 St. Petersburg, Russia*

[§] *Aix Marseille Univ., CNRS, CINAM, 13288 Marseille Cedex 9, France*

[‖]*Department of Engineering Physics, McMaster University, Hamilton, Ontario, Canada, L8S4L7*

ABSTRACT

Au droplets are used as a catalyst for the growth of nanowires on Si(111) substrate *via* the vapor-liquid-solid (VLS) mechanism. The dewetting of a Au thin film is the most common method to obtain these droplets. The control of this step is crucial to adjust the density and the diameter of the nanowires during VLS growth. When the Si(111) substrate is covered with a silicon dioxide layer, the kinetics of Au droplet formation is strongly modified. The dependence of the diameter and spatial distribution of the droplets on the surface have been studied by scanning electron microscopy with respect to the thickness of the silicon dioxide layer, the thickness of the Au film and the temperature of the substrate during deposition and post-deposition annealing. *In-situ* low energy electron microscopy and low energy electron diffraction revealed the dynamics of the Au droplet formation after annealing. The Au droplets are shown to catalyze the decomposition of silicon dioxide at high temperature (> 650-700 °C) and form a wetting layer of Au-($\sqrt{3}\times\sqrt{3}$)-Si(111). Consequently, the droplets absorb silicon atoms from the substrate, migrate perpendicular to the atomic steps and grow by the Smoluchowski ripening process.

1- INTRODUCTION

Au-assisted growth of nanowires (NWs) based on different materials such as ZnO, GaAs, GaN, InGaAs, Si, Ge and InAs have been performed using many growth techniques: molecular beam epitaxy (MBE), metalorganic vapor phase epitaxy (MOVPE) and hydride vapor phase epitaxy (HVPE).[1–3] The Au droplets act as a mediator between the growth precursors and the solid NW phase. In VPE methods, the Au droplets have also a catalytic role; i.e., they assist in the decomposition of the precursors on their surface. The Au droplets subsequently collect and accumulate atoms, which are deposited as a solid phase at the substrate-droplet interface once saturation is reached inside the droplet. Depending on the temperature, different growth mechanisms can occur: the vapor-liquid-solid (VLS) process where the catalyst metallic droplet is liquid during NW growth,[4,5] and the vapor-solid-solid (VSS) process where the growth occurs *via* solid metallic catalyst droplets.[6] In both cases, the diameters and the position of the resulting NWs on the surface are pre-defined by the size and distribution of the Au catalysts. Thus, the control of the morphology and the spatial distribution of the Au droplets on the substrate are crucial.

Several methods are used to control the Au droplet deposition. The spin coating of a colloidal solution containing Au nanoparticles and the dewetting of ultra-thin metallic films are the most common methods. The latter approach has been an important topic in material science and technology.[7–12] The high surface-to-volume ratio of these films may produce a high driving force for dewetting, which tends to agglomerate matter to reduce the total surface/interface energy of the system.[13,14] Consequently, the size distribution of the droplets is determined by the kinetics of mass transfer that depends on many parameters such as the temperature, the film thickness and the substrate chemical nature, orientation and roughness. Solid state dewetting and ripening have been mostly studied and described in non-reactive systems,[15] whereas chemical reactions between the film and the substrate may occur and lead to complex behaviors such as triple line pinning at reactive fronts [15] or modification of wetting properties by alloying phenomena[16]. In previous work,[17] we demonstrated that GaAs NW growth *via* the VLS-HVPE mechanism mediated by Au droplets on bare Si(111) substrate was ineffective whereas a high density of structures nucleate and grow on oxidized Si(111) substrate. We assumed that, in addition to its role of forming pinning sites for catalyst droplets,[18–20] the presence of the oxide layer acts as a barrier against the absorption of silicon atoms from the substrate at high growth temperatures. It is the aim of the present work

to unravel more precisely the role of this oxide layer on the droplet dynamics at the surface, and to determine the most appropriate conditions of Au droplets formation for subsequent NW growth with VPE methods.

We have investigated the agglomeration dynamics of an ultra-thin Au film on Si(111) substrates when covered by a silicon dioxide (SiO_2) layer. The density and size distribution of the Au droplets at the surface were characterized with respect to the thickness of the Au film and oxide layer, temperature of deposition, and post-deposition annealing. Real time *in-situ* measurements by low energy electron microscopy have revealed the interplay between the decomposition of the SiO_2 layer favored by the Au droplets and the droplet growth *via* static and dynamic coalescence. The phenomena of Au droplet pinning and Si substrate dissolution on the surface are discussed. The improved understanding of the Au dewetting mechanisms provided in this paper is not only useful for NW growth, it can be of interest for a wide range of applications.[21,22]

2- EXPERIMENTAL

Three types of sample were used in this study, all fabricated using (111) n-doped silicon wafers (1 Ω.cm) but with different oxide layers: (1) a native oxide of thickness ~ 1.2 nm and a surface roughness of 0.55 nm RMS, (2) a 5 nm-thick thermal oxide of surface roughness ~ 0.35 nm RMS, grown by dry oxidation method after a chemical etching of the native oxide (by dipping in 1% HF solution for 3 minutes) and (3) a 500 nm-thick thermal oxide of surface roughness less than 0.3 nm as estimated by the supplier (SIL'TRONIX). The native oxide thickness was estimated by X-ray photoelectron spectroscopy (XPS).

Au film deposition and post-deposition annealing were performed in ultra-high vacuum (UHV) with a base pressure of $\sim 10^{-7}$ Pa. Au (purity of 99.9998%) was deposited by a Knudsen cell at a rate of about 0.02 $nm \cdot min^{-1}$. The deposition rate was determined by several Au deposition/XPS measurement cycles as shown in Ref. [23].

Scanning electron microscopy (SEM) was used to characterize the samples after growth or annealing, while the dynamics of the Au droplets during annealing was studied by *in-situ* low energy electron microscopy (LEEM) coupled with low energy electron diffraction (LEED). The SEM images were taken in a Zeiss Supra 55VP field emission scanning microscope with in-lens detection mode at a working distance of 5.5 mm and an incident energy of 3 kV. *Ex-situ* non-

contact AFM (PSIA-XE 100) was used to characterize the sample topography. *In-situ* measurements (LEEM and LEED) were performed in an UHV chamber equipped with an Elmitec LEEM III microscope.[24] The observations were carried out in bright field mode, with electron beam energy of 3 eV. Sequential images were recorded at a rate of 1 Hz. This allowed for a good compromise between image quality and real-time acquisition. Diffraction patterns of the surface were taken by LEED (electron beam energy of 15 eV).

3- RESULTS AND DISCUSSION

Many experimental parameters may influence the size and spatial distribution of Au droplets on the surface. In the following, we discuss the effects of (i) oxide thickness and substrate temperature, (ii) Au film thickness and (iii) annealing time.

To examine the effect of the temperature on the spatial distribution of Au droplets, the equivalent of 1 nm (4 monolayers (ML)) of Au was deposited at room temperature (RT), and at 600 °C on oxidized surfaces (native oxide, 5 nm and 500 nm thermal oxides). For the samples processed at 600 °C, the substrate temperature was cooled down to RT directly after Au deposition. SEM images showing the spatial distributions of Au morphology are given in Figure 1. After deposition at RT, the density and size distribution of Au droplets on all samples are very similar (Figure 1a-c) regardless of the oxide thickness. On the other hand, the deposition at 600 °C results in different behavior for the three samples. The density and the size distribution decrease considerably when increasing the SiO_2 thickness (Figure 1d-f). This is likely related to an enhanced diffusion of Au droplets on thicker SiO_2 layers where the roughness, and therefore the developed surface and the morphological defects, are considerably reduced. Thus, Au atoms on thick SiO_2 surfaces at high temperature can diffuse at larger distances before forming larger clusters.

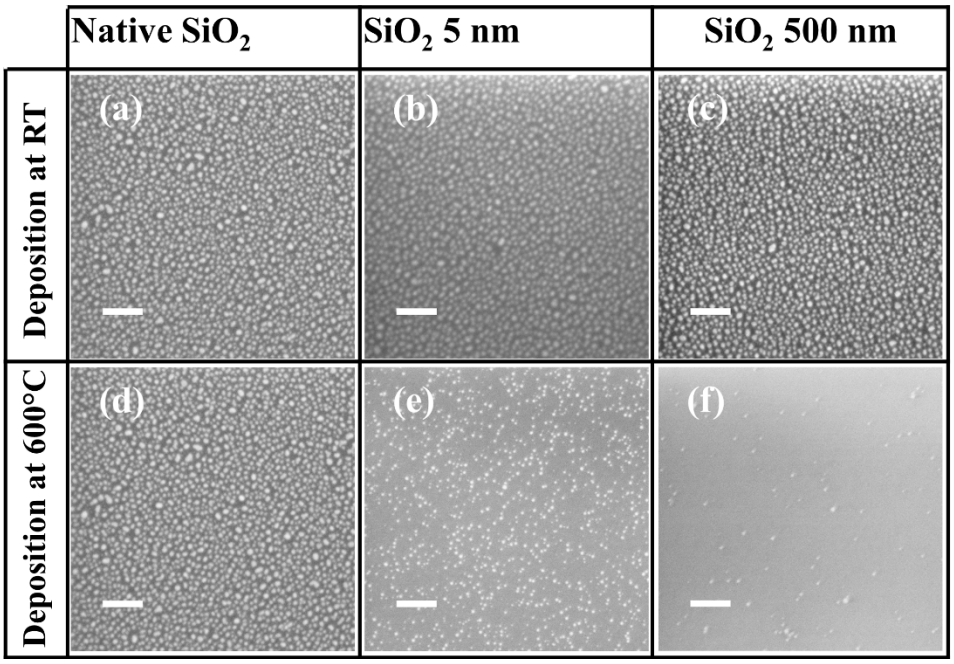

Figure 1: SEM images showing the distribution of as-deposited Au after evaporation of 1 nm of Au at RT (upper row) and 600 °C (lower row) on different types of substrate: (a and d) native oxide, (b and e) 5 nm-thick oxide, and (c and f) 500 nm-thick oxide. Scale bar = 100 nm.

The high diffusivity of Au at 600°C on 500 nm-thick thermal oxide prevents the formation of nanometer-size Au droplets that are desirable for NW growth (NW growth temperature by HVPE is above 600 °C). Thus, we have chosen Si(111) substrates with native oxide and 5 nm-thick thermal oxide to study the effect of the Au film thickness (from 0.2 to 2 nm) on the droplet formation kinetics. The Au films were deposited at RT, and subsequently annealed at 600 °C for 10 minutes in UHV. The SEM images of Figure 2 indicate an increase of the droplet size and decrease of the droplet density with Au film thickness (h_{Au}). For h_{Au}= 2 nm deposited on native SiO_2, SEM images (Figure 2d) reveal a bimodal droplet size distribution. The largest droplets appear with irregular shapes surrounded by depleted zones. These droplets also have a darker contrast with respect to the smallest ones that may be attributed to a change of chemical composition. From these measurements, we attribute the irregular droplet formation to the local decomposition of the oxide layer, allowing the Au droplets to spread onto the Si(111) surface and absorb silicon to reach the liquidus composition (~30% Si at 600 °C [27]). This will be studied in more detail in the second part of this paper. No irregular droplets were observed on the 5 nm-thick

thermal oxide, suggesting that the oxide layer was probably not entirely decomposed (as expected, a thicker SiO_2 layer requires more time to be decomposed).

The nucleation probability of NWs is considerably reduced by the presence of Si in the Au droplets.[17] Therefore, the substrates that have decomposed SiO_2 layers are not suitable for NW growth. Consequently, we have focused on the native oxide substrate and deposited only 1 nm of Au. This ensures the formation of an adequate density of small pure Au droplets when annealed at 600 °C.

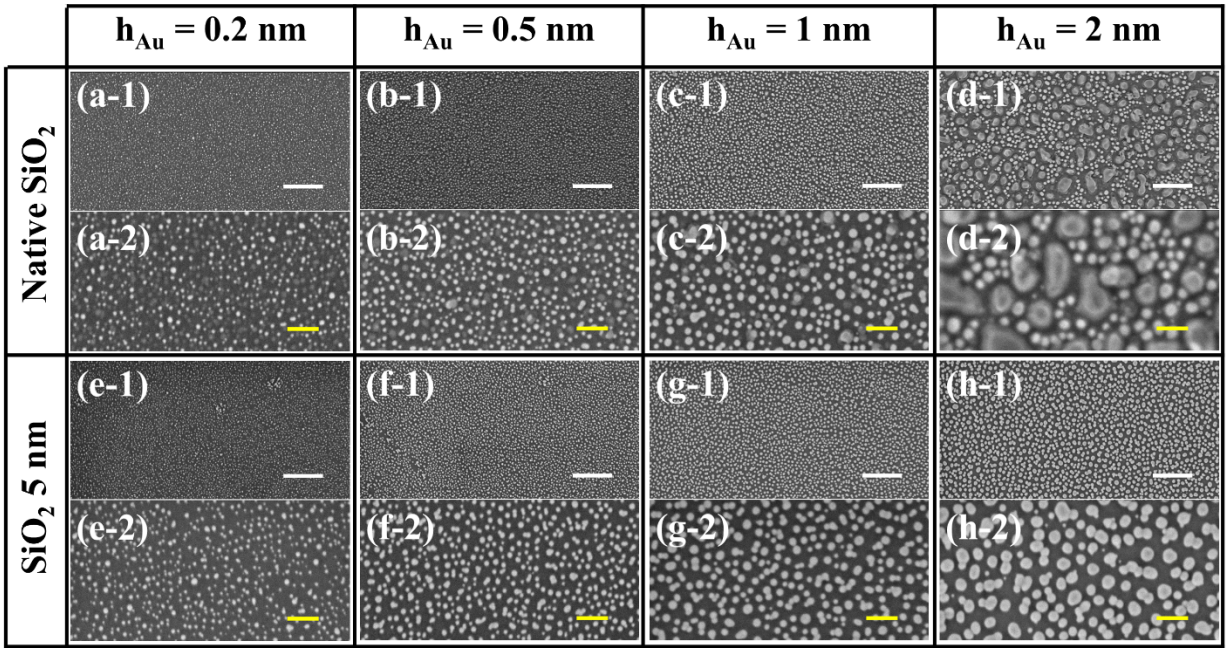

Figure 2: SEM images showing the distribution of Au droplets after deposition of (a,e) 0.2, (b,f) 0.5, (c,g) 1 and (d,h) 2 nm of Au at RT followed by annealing at 600 °C for 10 minutes under UHV. The upper two rows correspond to samples with native SiO_2 and the bottom two rows correspond to samples with 5 nm thick thermal oxide. The white and yellow scale bars represent 200 nm and 50 nm, respectively.

Next, sequential characterization of the surface topography was performed for different annealing times. This is given in Figure 3. The SEM images of Figure 3f-j show that the mean droplet size increased with annealing duration. The evolution of the droplet size distributions is indicated in Figure 3a-e. Initially, the as-deposited droplets have a Gaussian diameter distribution (distribution 1) with a narrow full-width-at-half-maximum (FWHM) and a mean diameter of 10

nm (Figure 3f). We have reported previously that as-deposited droplets have an average height of ~2.2 nm.[23] At t_a=30 min (Figure 3h), the mean size increases slightly and the FWHM becomes larger. This behavior indicates that large stable droplets grow at the expense of smaller ones to decrease the total surface to volume ratio of the droplets.[28–30] However, at t_a=60 min, a change of behavior occurs where large droplets with irregular shapes start to appear, as shown by the distribution 2 in Figure 3d,e. This behavior is similar to the one described earlier for a 2 nm thick Au film at t_a=10 min, and was attributed to the oxide layer decomposition. We conclude that the same phenomenon occurs at later times (t_a=60 min) if a smaller amount of Au (h_{Au}=1 nm) is deposited. Figure 4 shows the evolution of the droplet density (number of droplets μm^{-2}) and the fraction of area covered with droplets (coverage) with annealing time. These quantities are measured using the SEM images of Figure 3f-j. The colors of the points in Figure 4 correspond to those used for the distributions in Figure 3a-e. Clearly, the droplet density decreases with increasing t_a due to the coalescence of small droplets. The coverage also decreases with t_a indicating that the droplets formed by coalescence reshape to get closer to the equilibrium shape by reducing their footprint area at the surface. Note that a simple evaluation combining the coverage obtained in Figure 4 and XPS measurement shows that the total amount of gold remains stable up to 30 min of annealing, revealing that Au evaporation is unlikely to be efficient.

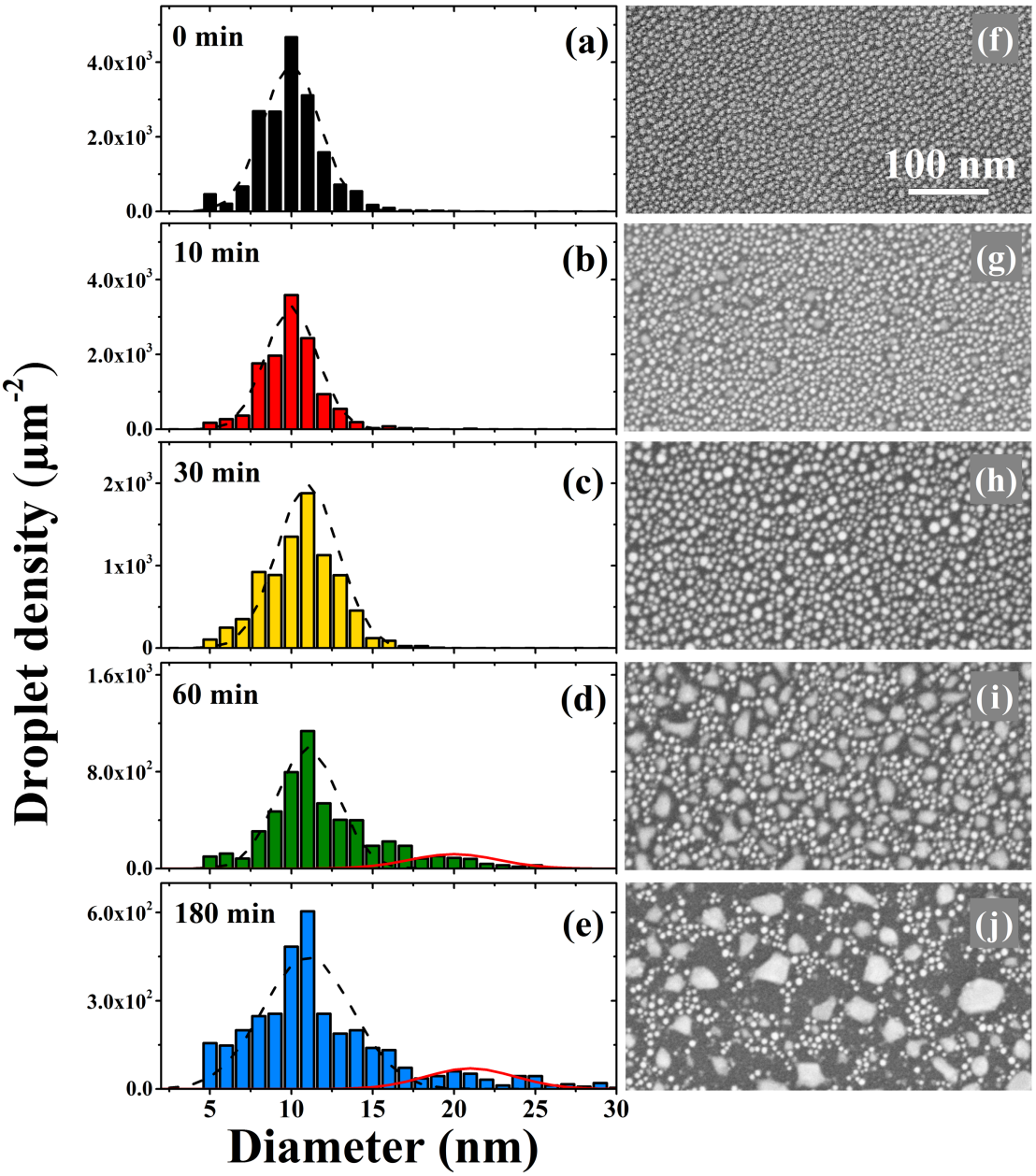

Figure 3: Distribution of Au droplets after deposition at RT and annealing at 600 °C of 1 nm of Au on the native oxide substrate for different annealing times t_a: (a) 0, (b) 10, (c) 30, (d) 60 and (e) 180 minutes. The black-doted and the red distributions represent respectively distribution 1 and distribution 2 discussed in the text. The right panels are the *ex-situ* SEM images and the left ones are the size distributions of the droplets. After 60 minutes of annealing, a bimodal distribution appears, indicating a partial decomposition of the SiO_2 layer beneath the large droplets and the formation of a Au-Si alloy after absorbing Si atoms from the substrate.

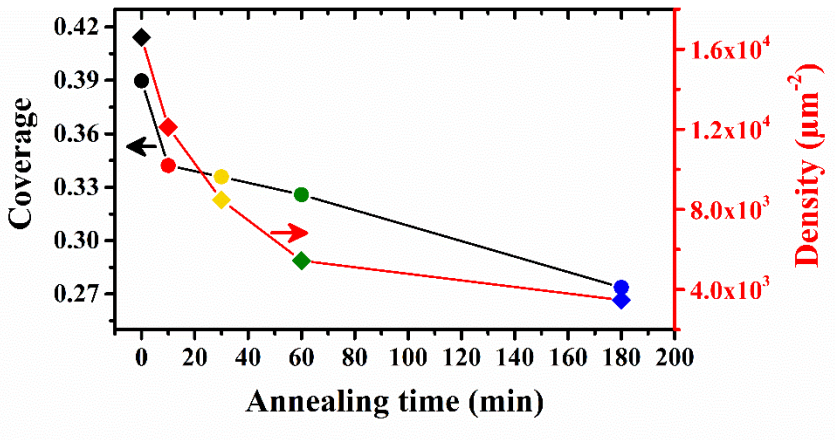

Figure 4: Density of droplets and surface coverage as function of the annealing time. The colors of the data points correspond to those used for the distributions in Figure 3.

The metal-promoted reactions of silicon depend strongly on temperature. They are complex but widely studied.[31,32] To further study the kinetics of oxide decomposition and Au droplet formation, *in-situ* LEEM coupled with LEED was used. Figures 5 (panels a to c) show the time evolution of the surface under annealing at 700 °C. The Au amount deposited is 1 nm, and the substrate is the same as the native oxidized one used above. The time t = 0 s corresponds to the stage where the droplets (dark contrast) become sufficiently large to be distinguished clearly at the surface. During the annealing, the droplets grow and migrate on the surface (as shown in Figure 3), forming behind them bright regions. These regions, characterized by micro-LEED (beam spot diameter 300 nm), have a hexagonal pattern (Figure 5e) that is characteristic of the Au-($\sqrt{3}\times\sqrt{3}$)-Si(111) surface reconstruction.[26, 27] The existence of this surface reconstruction shows that the amorphous SiO_2 layer is locally completely etched. Note that the same results can be extrapolated to lower temperatures (~ 600 °C), except that much longer annealing time would be required. In addition to the oxide decomposition mediated by Au droplets, a strong decrease of the droplet density occurs at the surface. Figure 5d shows the evolution of the number of Au droplets per unit area with time. The fit shows an exponential decay with a typical time scale τ=190±10 s. This decay cannot be attributed to conventional Ostwald ripening ($N(t)\sim t^{-3/4}$) that is much too slow.[29] Smoluchowski ripening partially explains the droplet density decay.[35] Indeed, the largest droplets move spontaneously by lateral migration towards the silicon while etching the surrounding silica and grow fast by capturing neighboring droplets (see LEEM *in-situ* movie in Supporting Information). LEEM real-time measurements also show that after the passage of the migrating

droplets, the Au-reconstructed areas appear as perfectly flat since no atomic step edge can be detected. The AFM images in Figure 6a corroborate this result: the surface is flattened by the droplet migration. As shown on bare Si(111) surface, the directed motion of the droplets is driven by the step structure of the underlying Si(111) substrate.[33] As the surface below the oxide was initially vicinal, Au droplets that decompose the oxide climb up the staircase to efficiently absorb Si and reach the liquidus composition (~35% Si at 700 °C). This explains the preferential direction to the Au migration and track formation seen in Figure 5a-c. The track profiles (Figure 6c) behind the droplets show that the slope is locally about 0.1±0.02° misaligned with respect to the average plane of the surface. This angle is compatible with the miscut angle of the Si(111) surface and indicates that the Si steps have been dissolved by the Au-Si droplets. However, the main mechanism for the droplet density decrease is the spontaneous decay of the smallest Au droplets. Droplets decay abruptly by edge retraction and this mechanism can be assigned to an unpinning phenomena of the triple-line SiO_2-Si-Au(droplet) that initiates the motion. The driving force for unpinning is, however, difficult to assess. At 700°C Au in the Au-Si alloy droplets may slowly evaporate or dissolve into the oxide layer and Si bulk. Moreover, droplets are in competition with the Au-($\sqrt{3}\times\sqrt{3}$)-Si(111) surface reconstruction that needs also to consume 1 ML of Au to cover the whole surface. *Ex-situ* AFM measurements of the droplet morphology allows an estimation of the wetting angle θ of the droplets (Figure 6b and Figure 6d). The AFM tips are made of Si with a conic shape (angle <40°) and a typical radius of curvature of 8 nm. Assuming a spherical shape, the wetting angle θ is about 155±10°, which is larger than that expected on the Si(111) surface.[16] This result suggests Au-Si alloy droplets pinned at the triple-line SiO_2-Si-Au(droplet) due to Au loss decay in height. This height reduction induces a force for the unpinning of the droplet edge that initiates the decay.

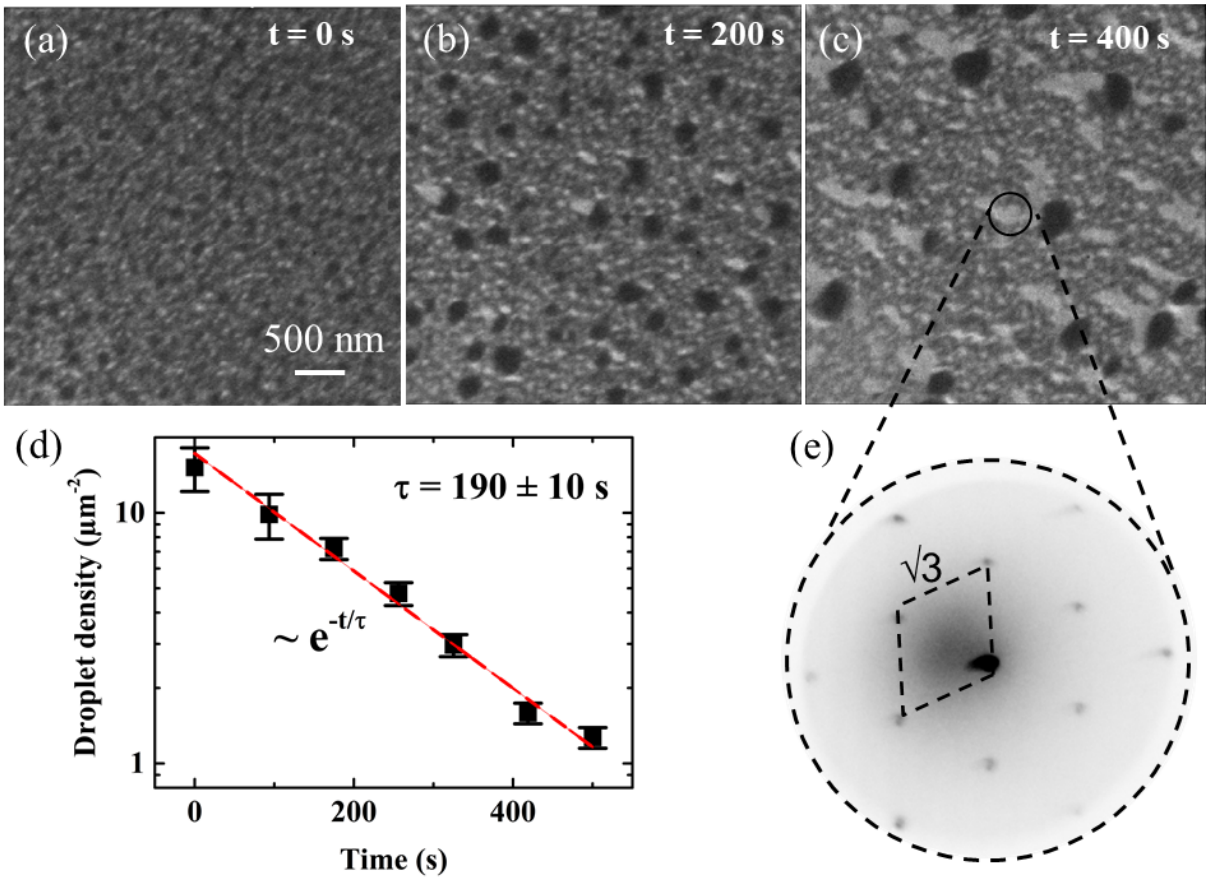

Figure 5: (a)-(c) LEEM images showing the evolution of the Au droplet growth and migration on the surface while decomposing the native SiO_2 at 700 °C. The thickness of Au is 1 nm, deposited at RT before annealing. For the complete movie see Supporting Information. (b) Droplet density as a function of time (squares) and exponential fit (red dashed line). (c) LEED pattern of the tracks formed behind the migrating droplet. The surface exhibits a Au-($\sqrt{3}\times\sqrt{3}$)-Si(111) reconstruction.

1

2

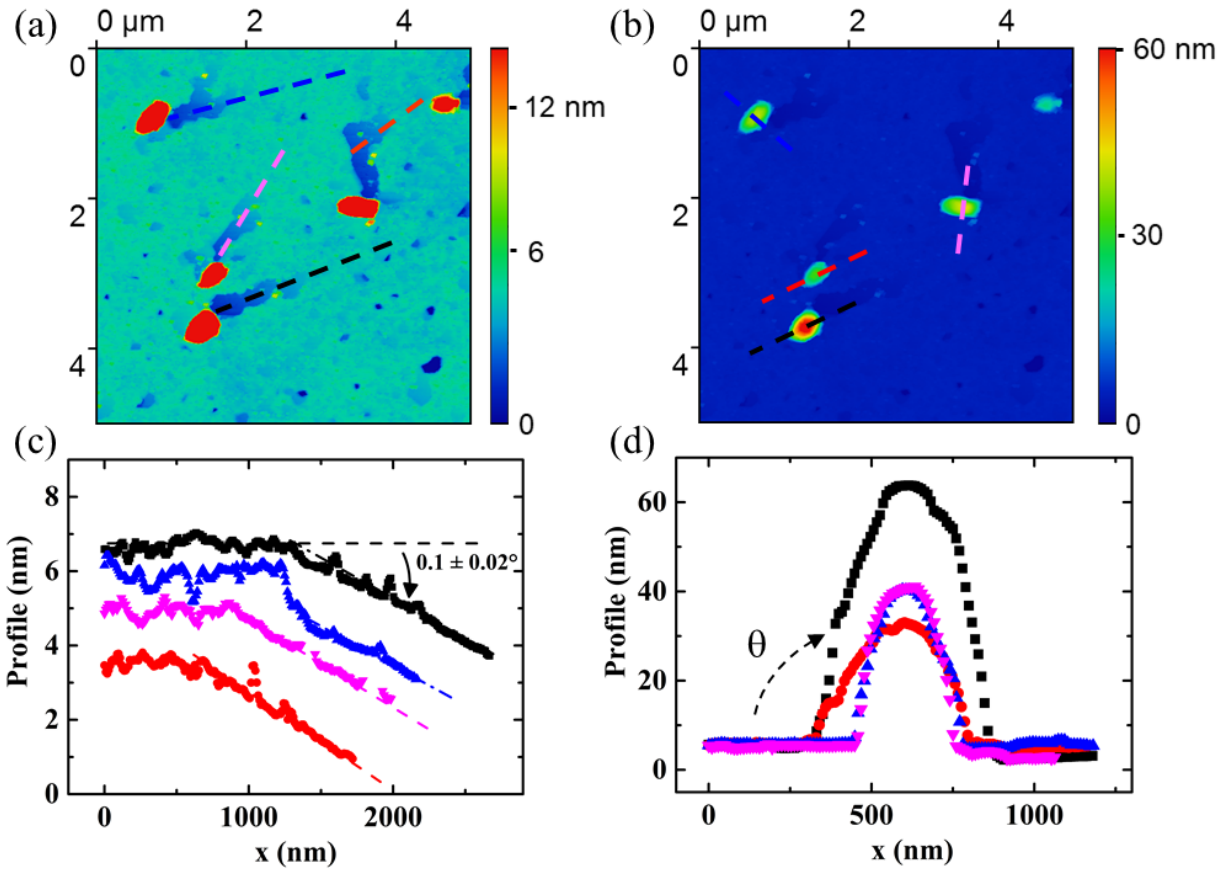

Figure 6: (a) AFM images showing the etching of the SiO_2 layer by migration of the Au droplets. The tracks behind the droplets show the Si(111) substrate with the Au-($\sqrt{3}\times\sqrt{3}$)-Si(111) surface reconstruction.(b) Same as (a) but with extended height scale to show the droplet morphology. (c)-(d). Height profiles along the dashed lines in (a) and (b), respectively.

Considering these *in-situ* observations and results obtained by SEM (Figure 2 and 3), the mechanisms of Au droplet formation and SiO_2 layer decomposition can be summarized as follows:

(i) At 600 °C-700 °C, a thin film of Au agglomerates into droplets that grow. After an incubation time for Au atoms to pass through the SiO_2 layer (depending on temperature and Au film thickness), the decomposition of the oxide layer is initiated. As reported elsewhere,[15,31] the presence of metal atoms (including Au) at the SiO_2/Si interface catalyzes the oxide decomposition by lowering the temperature of the reaction (800-900 °C without metal impurities). This process continues until the full decomposition of the oxide layer underneath the droplets.

(ii) After the oxide decomposition, the Au droplets start to absorb Si atoms from the substrate forming a Au-Si alloy that is liquid at $T \geq 370$ °C.[32,36] Therefore, the droplets tend to spread at the surface as wetting is more favorable on Si than on SiO_2.

(iii) To reach the liquidus composition, the largest droplets unpin from the initial site and migrate in the upward direction of the steps and absorb Si atoms by consuming the step edge. This process favors dynamic coalescence of the droplets. Meanwhile, the smallest droplets are unstable and decay spontaneously.

4- CONCLUSION

In conclusion, we have presented a study of the agglomeration dynamics of ultra-thin Au films on oxidized Si(111) substrates. When Au is deposited at RT, there is no effect of the oxide thickness on the size distribution and the density of the droplets. Under annealing in the range of 600-700 °C, two behaviors are predominant. On thick thermal oxides, Au diffusivity is strongly enhanced and prevents the formation of nanometer size Au droplets. For thermal SiO_2 layers, the decomposition of the oxide is activated by the Au atoms and this process modifies the Au droplet growth. Irregular-shape droplets start to appear after a sufficient annealing time, which is larger for smaller Au thickness deposited. This is attributed to the decomposition of the oxide layer and the absorption of Si atoms from the underlying substrate to form AuSi alloy. This process was studied *in-situ* by LEEM and LEED experiments supported by AFM measurements. We have shown that large Au droplets decompose the SiO_2 layer and unveil the Si(111) substrate while migrating perpendicular to the step edges. Small droplets are pinned and decay spontaneously. This study brings important information for NW growth using vapor phase epitaxy methods. Our results allow the control of the density and the diameters of the Au droplets for subsequent NW growth.

AUTHOR INFORMATION

Corresponding Authors

* Hadi Hijazi, ITMO University, Kronverkskiy pr. 49, 197101 St. Petersburg, Russia

E-mail: hadi.hijazi@uca.fr, hijazi@itmo.ru

Tel. : +33 (0) 6 60 37 32 65

SUPPORTING INFORMATION DESCRIPTION:

In-situ LEEM movie showing the evolution of the Au droplet growth and migration on the surface while decomposing the native SiO2 at 700 °C. The thickness of Au is 1 nm, deposited at RT before annealing. Total time 400 s. Electron energy: 3 eV. Field of view: 4.1 microns.

ACKNOWLEDGMENTS

This work has been supported financially by the CPER MMASYF of Region Auvergne-Rhone Alpes that we acknowledge gratefully. It was also funded by the program "Investissements d'avenir" of the French ANR agency, the French government IDEX-SITE initiative 16-µIDEX-0001 (CAP20-25), the European Commission (Auvergne FEDER Funds) and the Region Auvergne in the framework of the LabEx IMobS3 (ANR-10-LABX-16-01) and CPER. HH and VGD gratefully acknowledge the Russian Science Foundation for financial support under the Grant 19-72-30004. Electron microscopy was performed at the Canadian Centre for Electron Microscopy (also supported by NSERC and other government agencies). We also thank Alain Ranguis for AFM measurements.

REFERENCES

(1) Sharma, S.; Kamins, T. I.; Williams, R. S. Synthesis of Thin Silicon Nanowires Using Gold-Catalyzed Chemical Vapor Deposition. *Appl. Phys. A Mater. Sci. Process.* **2005**, *80*, 1225–1229.

(2) Orvatinia, M.; Imani, R. Effect of Catalyst Layer on Morphology and Optical Properties of Zinc-Oxide Nanostructures Fabricated by Carbothermal Evaporation Method. *Micro Nano Lett.* **2011**, *6*, 650.

(3) Joyce, H. J.; Gao, Q.; Tan, H. H.; Jagadish, C.; Kim, Y.; Fickenscher, M. A.; Perera, S.; Hoang, T. B.; Smith, L. M.; Jackson, H. E.; et al. Unexpected Benefits of Rapid Growth Rate for III-V Nanowires. *Nano Lett.* **2009**, *9*, 695–701.

(4) Gil, E.; Dubrovskii, V. G.; Avit, G.; André, Y.; Leroux, C.; Lekhal, K.; Grecenkov, J.; Trassoudaine, A.; Castelluci, D.; Monier, G.; et al. Record Pure Zincblende Phase in GaAs Nanowires Down to 5 nm in Radius. *Nano Lett.* **2014**, *14*, 3938–3944.

(5) Ramdani, M. R.; Gil, E.; Leroux, C.; André, Y.; Trassoudaine, A.; Castelluci, D.; Bideux, L.; Monier, G.; Robert-Goumet, C.; Kupka, R. Fast Growth Synthesis of GaAs Nanowires with Exceptional Length. *Nano Lett.* **2010**, *10*, 1836–1841.

(6) Lekhal, K.; Avit, G.; André, Y.; Trassoudaine, A.; Gil, E.; Varenne, C.; Bougerol, C.; Monier, G.; Castelluci, D. Catalyst-Assisted Hydride Vapor Phase Epitaxy of GaN Nanowires: Exceptional Length and Constant Rod-like Shape Capability. *Nanotechnology* **2012**, *23*, 405601.

(7) Kwon, J. Y.; Yoon, T. S.; Kim, K. B.; Min, S. H. Comparison of the Agglomeration Behavior of Au and Cu Films Sputter Deposited on Silicon Dioxide. *J. Appl. Phys.* **2003**, *93*, 3270–3278.

(8) Ruffino, F.; Pugliara, A.; Carria, E.; Romano, L.; Bongiorno, C.; Fisicaro, G.; La Magna, A.; Spinella, C.; Grimaldi, M. G. Towards a Laser Fluence Dependent Nanostructuring of Thin Au Films on Si by Nanosecond Laser Irradiation. *Appl. Surf. Sci.* **2012**, *258*, 9128–9137.

(9) Ruffino, F.; Grimaldi, M. G. Controlled Dewetting as Fabrication and Patterning Strategy for Metal Nanostructures. *Phys. Status Solidi Appl. Mater. Sci.* **2015**, *212*, 1662–1684.

(10) Thompson, C. V. Solid-State Dewetting of Thin Films. *Annu. Rev. Mater. Res.* **2012**, *42*,

399–434.

(11) Henley, S. J.; Carey, J. D.; Silva, S. R. P. Pulsed-Laser-Induced Nanoscale Island Formation in Thin Metal-on-Oxide Films. *Phys. Rev. B - Condens. Matter Mater. Phys.* **2005**, *72*, 1–10.

(12) Ruffino, F.; Grimaldi, M. G.; Bongiorno, C.; Giannazzo, F.; Roccaforte, F.; Raineri, V.; Spinella, C. Normal and Abnormal Grain Growth in Nanostructured Gold Film. *J. Appl. Phys.* **2009**, *105*, 2–8.

(13) De Gennes, P. G. Wetting: Statics and Dynamics. *Rev. Mod. Phys.* **1985**, *57*, 827–863.

(14) Bonn, D.; Eggers, J.; Indekeu, J.; Meunier, J. Wetting and Spreading. *Rev. Mod. Phys.* **2009**, *81*, 739–805.

(15) Leroy, F.; Passanante, T.; Cheynis, F.; Curiotto, S.; Bussmann, E. B.; Müller, P. Catalytically Enhanced Thermal Decomposition of Chemically Grown Silicon Oxide Layers on Si(001). *Appl. Phys. Lett.* **2016**, *108*, 111601.

(16) Ressel, B.; Prince, K. C.; Heun, S.; Homma, Y. Wetting of Si Surfaces by Au-Si Liquid Alloys. *J. Appl. Phys.* **2003**, *93*, 3886–3892.

(17) Hijazi, H.; Dubrovskii, V. G.; Monier, G.; Gil, E.; Leroux, C.; Avit, G.; Trassoudaine, A.; Bougerol, C.; Castellucci, D.; Robert-Goumet, C.; André, Y. Influence of Silicon on the Nucleation Rate of GaAs Nanowires on Silicon Substrates. *J. Phys. Chem. C* **2018**, *122*, 19230-19235.

(18) Colombo, C.; Spirkoska, D.; Frimmer, M.; Abstreiter, G.; Fontcuberta i Morral, A. Ga-Assisted Catalyst-Free Growth Mechanism of GaAs Nanowires by Molecular Beam Epitaxy. *Phys. Rev. B* **2008**, *77*, 155326.

(19) Fontcuberta i Morral, A.; Colombo, C.; Abstreiter, G.; Arbiol, J.; Morante, J. R. Nucleation Mechanism of Gallium-Assisted Molecular Beam Epitaxy Growth of Gallium Arsenide Nanowires. *Appl. Phys. Lett* **2008**, *92*, 1–4.

(20) Wagner, R. S.; Ellis, W. C. Vapor-Liquid-Solid Mechanism of Single Crystal Growth. *Appl. Phys. Lett.* **1964**, *4*, 89.

(21) Ruffino, F.; Grimaldi, M. G.; Giannazzo, F.; Roccaforte, F.; Raineri, V. Nanoscale Voltage Tunable Tunnel Rectifier by Gold Nanostructures Embedded in SiO2. *Appl. Phys. Lett.* **2006**, *89*, 3–6.

(22) Temple, T. L.; Bagnall, D. M. Optical Properties of Gold and Aluminium Nanoparticles for

Silicon Solar Cell Applications. *J Appl. Phys.* **2011**, *109*, 84343.

(23) Mahjoub, M. A.; Monier, G.; Robert-Goumet, C.; Bideux, L.; Gruzza, B. XPS Combined with MM-EPES Technique for in-situ Study of Ultra Thin Film Deposition: Application to an Au/SiO2/Si Structure. *Appl. Surf. Sci.* **2015**, *357*, 1268–1273.

(24) Cheynis, F.; Leroy, F.; Ranguis, A.; Detailleur, B.; Bindzi, P.; Veit, C.; Bon, W.; Müller, P. Combining Low-Energy Electron Microscopy and Scanning Probe Microscopy Techniques for Surface Science: Development of a Novel Sample-Holder. *Rev. Sci. Instrum.* **2014**, *85*, 043705.

(25) Shi, Z.; Shao, S.; Wang, Y. Improve the Surface Roughness of Silicon Nanophotonic Devices by Thermal Oxidation Method. *J. Phys. Conf. Ser.* **2011**, *276*, 012087.

(26) Levine, J. R.; Cohen, J. B.; Chung, Y. W. Thin Film Island Growth Kinetics: A Grazing Incidence Small Angle X-Ray Scattering Study of Gold on Glass. *Surf. Sci.* **1991**, *248*, 215–224.

(27) Gerlach, W.; Goel, B. Gold Silicon Phase Diagram. *Solid State Electron.* **1967**, *10*, 589–592.

(28) Chakbavebty, B. K. Grain Size Distribution in Thin Films-1. Conservative Systems. *J. Phys. Chem. Solids* **1967**, *28*, 2401–2412.

(29) Fischmeister, H.; Grimvall, G. Ostwald Ripening - A Survey. In *Sintering and Related Phenomena*; Kuczynski, G. C., Ed.; Plenum Press: New York, 1973; pp 119–149.

(30) Ruffino, F.; Canino, A.; Grimaldi, M. G.; Giannazzo, F.; Bongiorno, C.; Roccaforte, F.; Raineri, V. Self-Organization of Gold Nanoclusters on Hexagonal SiC and SiO2 Surfaces. *J. Appl. Phys.* **2007**, *101*, 0–7.

(31) Dallaporta, H.; Liehr, M.; Lewis, J. E. Silicon Dioxide Defects Induced by Metal Impurities. *Phys. Rev. B* **1990**, *41*, 5075–5083.

(32) Hiraki, A.; Lugujjo, E.; Mayer, J. W. Formation of Silicon Oxide over Gold Layers on Silicon Substrates. *J. Appl. Phys.* **1972**, *43*, 3643.

(33) Curiotto, S.; Leroy, F.; Cheynis, F.; Müller, P. Self-Propelled Motion of Au-Si Droplets on Si(111) Mediated by Monoatomic Step Dissolution. *Surf. Sci.* **2015**, *632*, 1–8.

(34) Curiotto, S.; Leroy, F.; Cheynis, F.; Müller, P. In-Plane Si Nanowire Growth Mechanism in Absence of External Si Flux. *Nano Lett.* **2015**, *15*, 4788–4792.

(35) Smoluchowski, M. V. Brownsche Molekularbewegung Und Koagulation von

Kolloidteilchen. *Phys. Zeits.* **1916**, *17*, 585–599.

(36) Rath, A.; Dash, J. K.; Juluri, R. R.; Rosenauer, A.; Schoewalter, M.; Satyam, P. V. Growth of Oriented Au Nanostructures: Role of Oxide at the Interface. *J. Appl. Phys.* **2012**, *111*, 16–19.

TOC Graphic:

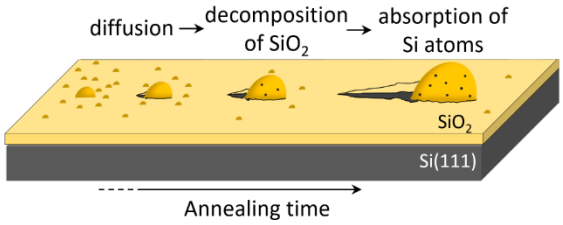
diffusion
decomposition of SiO_2
absorption of Si atoms
SiO_2
Si(111)
Annealing time